Reliability Evaluation of Multichip Phase-Leg IGBT Modules Using Pressureless Sintering of Nanosilver Paste by Power Cycling Tests

Shancan Fu, Yunhui Mei*, *Member, IEEE*, Xin Li, Changsheng Ma, and Guo-Quan Lu*, Member, IEEE*

***Abstract*—Nanosilver paste has become a promising lead-free die-attach material for power electronic packaging. This development solves the challenges faced by power device manufacturers to replace the lead-based or lead-free solders for high-temperature applications. This paper proposes the reliability of a 1200-V/150-A multichip insulated-gate bipolar transistor (IGBT) module using pressureless sintering of nanosilver paste as die attachment. The degradation in harsh environment was compared between the proposed IGBT module using pressureless sintered nanosilver and the commercial one using Sn5Pb92.5Ag2.5 solder by power cycling with two different test conditions. The device junction-to-case thermal resistance, *I–V* characteristics, and switching performance were measured at various numbers of cycles. The results show that the pressureless sintered nanosilver, which was used as the die attachment of the multichip phase-leg IGBT modules, has superior reliability rather than the commercial one.**

***Index Terms*—Electrical properties, insulated-gate bipolar transistor module, power cycling, pressureless sintering, silver nanoparticles, thermal resistance.**

I. Introduction

NOWADAYS, insulated-gate bipolar transistors (IGBTs) have been widely used in numerous applications, including the traditional industrial systems, e.g., converter devices, power and traction drive systems, and the new application systems, e.g., renewable energy development and electric vehicles [1]–[3]. However, the IGBT module also faces with some challenges with the pressure to decrease the size of power electronics systems so that some IGBT module footprint area is reduced by 50%. This has resulted in higher power dissipation densities for the IGBTs due to denser packing of the whole structure. In addition, the high switching frequencies and high voltage of IGBTs also result in higher power dissipation at the die level.

In the last decades, many efforts had been made to increase the power density and heat dissipating capacity of the IGBT modules. Li *et al.* [4] propose a novel packaging design based on the concept of N-cell and P-cell to directly reduce the stray inductance inside of an IGBT power module. Compared with commercial modules, this novel method was expected to reduce the inductance by 50%. Mirzaee *et al.* [5] designed IGBT modules with SiC diodes instead of traditional Si diodes. It shows that the IGBT module with SiC diode shows less switching loss than the one with Si diode, particularly at higher switching speed and lower gate resistance due to prevention of reverse-recovery-induced loss mechanisms. Hensler *et al.* [6] tried to use the low-temperature joining technique (LTJT) to join the power chips instead of traditional solder reflowing. The power modules using the LTJT shows excellent reliability compared to standard ones. However, all of these reported power modules by LTJT were in use of auxiliary pressure, which may crack the power chips and still complicate the manufacturing process. Recently, we added some specific organics in the nanosilver paste to increase the chemical driving force instead of mechanical one, which could get rid of the auxiliary pressure for low-temperature sintering of nanosilver paste [7]. Then, we bonded large-area Si-based IGBT chips with direct-bonded-copper (DBC) substrate by pressureless sintering of nanosilver paste. The electrical and switching characteristics of the IGBT module with pressureless sintered nanosilver show comparable performance with those of high-temperature solder, i.e., Sn5Pb92.5Ag2.5.

Besides the performance, the reliability of the IGBT module is also an important item that both manufacturers and users extremely care. The reliability of IGBT module mainly depends on the thermal stress caused by the material mechanical deformation, which is a heat and mechanical process [8]. During the operation, the total power, losses including switching loss, conduction loss, and leakage current loss, could cause the junction temperature rise greatly. The device constantly endures temperature swings during the operation. IGBT module is usually with a multilayer architecture that is assembled by different materials, e.g., silicon, solders, copper, and ceramic. During the temperature cycling, these materials are subjected to compression or tensile stresses because of the mismatch of their

Manuscript received May 10, 2016; revised August 29, 2016; accepted October 10, 2016. Date of publication October 19, 2016; date of current version March 24, 2017. This work was supported in part by the National High Technology Research and Development Program of China (2015AA034501) and in part by the Tianjin Municipal Natural Science Foundation (13ZCZDGX01106). Recommended for publication by Associate Editor F. Wang. *(Corresponding author: Yunhui Mei.)*

S. Fu, Y. Mei, and X. Li are with the Tianjin Key Laboratory of Advanced Joining Technology and School of Material Science and Engineering, Tianjin University, Tianjin 300072, China (e-mail: fushancan@163.com; yunhui@tju.edu.cn; xinli@tju.edu.cn).

C. Ma is with Jiangsu Macro and Micro Technology Co., Ltd, Changzhou 215008, China (e-mail: csma@macmicst.com).

G.-Q. Lu is with the School of Materials Science and Engineering, Tianjin University, Tianjin 300072, China, and also with the Department of Materials Science and Engineering and Bradley Department of Electrical and Computer Engineering, Virginia Polytechnic Institute and State University, Blacksburg, VA 24061 USA (e-mail: gqlu@vt.edu).

Color versions of one or more of the figures in this paper are available online at http://ieeexplore.ieee.org.

Digital Object Identifier 10.1109/TPEL.2016.2619118

See http://www.ieee.org/publications_standards/publications/rights/index.html for more information.

thermal expansion coefficients (CTE) [9]. As a result, the stresses could destroy any joint in the power module potentially, e.g., die attachment and wirebond, resulting in the module failure. Ji *et al.* [10] have studied the multiobjective design optimization of IGBT power modules to improve reliability and prolong lifetime. The multiobjective optimization strategy was designed considering different failure mechanisms, e.g., material degradation, fatigues by temperature cycling, power cycling, and vibration. Özkol *et al.* [11] had studied the HiPak modules using heavy ribbon bonding instead of the standard wire bonding as emitter interconnection. It was found that the lifetime of power cycling of the HiPak modules with the heavy ribbon bonding was improved up to four times compared to the standard modules using wire bonding. Kim *et al.* [12] had replaced traditional Al_2O_3-DBC substrate with AlN-DBC substrate because of its higher thermal conductivity to reduce the rise of junction temperature by power loss, leading the lower thermomechanical stress and better reliability consequently.

In addition, conventional solder reflowing had been widely used in electronic packaging [13]; however, they are susceptible to thermal fatigue and creep during long-term service, particularly at high temperatures [14], [15]. People then have also paid attention to study the reliability of power modules using different bonding techniques, e.g., transient liquid-phase (TLP) bonding and LTJT, for high-temperature applications. Yoon *et al*. [16] showed that the joint by the TLP had passed 1000 thermal cycles (−40 to 200 °C) without any significant delamination. Although TLP seems to be promising as a robust die-attach material, cost and reliability issues [17], [18] are the main deficiencies for wide usage.

The other approach is to use LTJT to attach power devices for high-temperature applications. Many people have studied the reliability of the mechanical properties of sintered silver joints, e.g., ratcheting fatigue failure [19], [20], visco-plastic deformation [21], and isothermal low cycle fatigue behavior [22]. For example, Chen *et al*. [23] claimed that sintered nanosilver joint has demonstrated a longer fatigue life and better response to shearing and cyclic loading than SAC305 joint, especially at high temperatures.

Recently, several research groups, e.g., Fraunhofer Institution, had reported the reliability of die attachment using sintered nanosilver by both power cycling tests [24]–[26] and thermal cycling tests [27], [28]. For example, Knoerr *et al.* [29] had compared the reliability of sintered nanosilver with two conventional solder alloys, i.e., Sn96.5Ag3Cu0.5 (SAC305) and Pb95Sn5. The lifetime of the sintered nanosilver could be up to 646 cycles by the thermal cycling test (−55 to 175 °C), while the lifetime of Pb95Sn5 solder and Sn96.5Ag3Cu0.5 solder was only 87 cycles and 51 cycles, respectively. It was concluded that nanosilver paste could be used as a promising lead-free die-attach material instead of high-lead or lead-free solder for power electronic packaging.

Furthermore, many other people had also evaluated the performance of the Si IGBT modules using nanosilver paste in the harsh environment, e.g., thermal impedance [30], electronics characteristics [31], [32]. For example, Cao *et al*. [33] showed that the thermal impedance of SAC305 samples and SN100C samples after 500 thermal cycles (−45 to 125 °C) was increased by 12.9% and 13.3%, respectively. The increment was much higher than that of the sample using the pressure-assisted sintered nanosilver, i.e., 3.1%. However, the previous studies were based on the sintering of nanosilver paste with assisted hydrostatic pressure, i.e., 5–10 MPa, which may damage the power chips during the packaging or complicate the processing. Pressureless sintering of nanosilver paste attracted more and more attention consequently. Although Zheng *et al*. [34] had reported that the die-shear strength of the pressureless sintered nanosilver on a copper substrate had not varied significantly and could still reach more than 30 MPa even after 1000 thermal cycles (−40 to 125 °C), the reliability of IGBT modules using the pressureless sintered nanosilver had been seldom reported before. We may concern the degradation of the IGBT modules using the pressureless sintered nanosilver because of lacking data and discussion on reliability tests, e.g., power cycling tests with various conditions.

In this paper, 1200-V/150-A half-bridge IGBT modules were demonstrated by pressureless sintering of the nanosilver paste to bond large-area IGBTs (12.56 mm × 12.56 mm) and diodes (6.3 mm × 6.3 mm). The objective is to compare the reliability of the multichip phase-leg IGBT modules using the pressureless sintered nanosilver with the ones using the high-lead solder, i.e., Sn5Pb92.5Ag2.5, by various power cycling tests, i.e., second-level and minute-level power cycling tests. The test conditions in details of the second-level and the minute-level power cycling tests are present in the text below. This paper was organized as follows: Section II described die attachment and package structure of the 1200-V/150-A IGBT modules; Section III evaluated the reliability of the IGBT modules using the pressureless sintered nanosilver and compared the reliability of the commercial ones using soldered Sn5Pb92.5Ag2.5.

II. Die Attachment and Package Structure

A. Die Attachment

Fig. 1 shows the comparison of the die-attach fabrication process using nanosilver paste and the commercial high-lead solder, i.e., Sn5Pb92.5Ag2.5 solder, respectively. The nanosilver paste was printed with a cross pattern on the DBC substrate. The cross pattern was designed to avoid trapping air bubbles inside the as-printed paste and also prevent the nanosilver paste overflow along the peripheral of die. Then, all the chips were mounted on the as-printed paste. In order to wet the interface well, the chips were pressed until the nanosilver paste was just squeezed out of the edges of the chips. The die attachment was first heated from the room temperature to 200 °C with a smooth ramping rate of 5 °C/min and maintained at 200 °C for 40 s. Then, the chips could be well bonded with a DBC substrate after sintering at 260 °C for 15 min. The die attachment of commercial IGBT modules used a high-lead solder, i.e., Sn5Pb92.5Ag2.5. The melting temperature of the solder is 280 °C, and the maximum processing temperature is 296 °C. The power chips can also be well bonded with a DBC substrate by vacuum reflowing [35].

Fig. 2 shows the comparison of void distribution in the die attachment of both pressureless sintered nanosilver and soldered Sn5Pb92.5Ag2.5. The void ratio in the soldered Sn5Pb92.5Ag2.5 layer, i.e., 2%–3%, was comparable as that

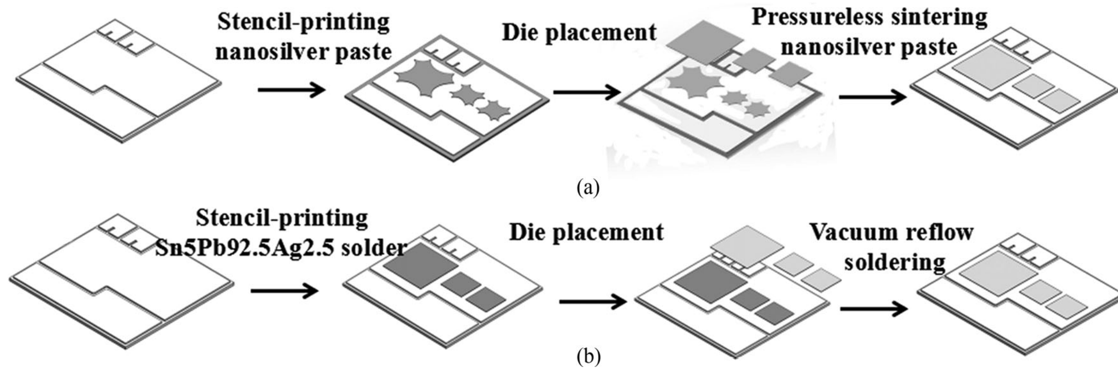

Fig. 1. Die-attaching process using (a) nanosilver paste and (b) Sn5Pb92.5Ag2.5 solder.

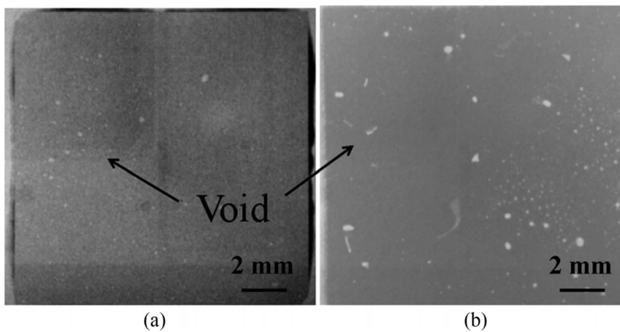

Fig. 2. Void distribution in (a) pressureless sintered nanosilver and (b) soldered Sn5Pb92.5Ag2.5.

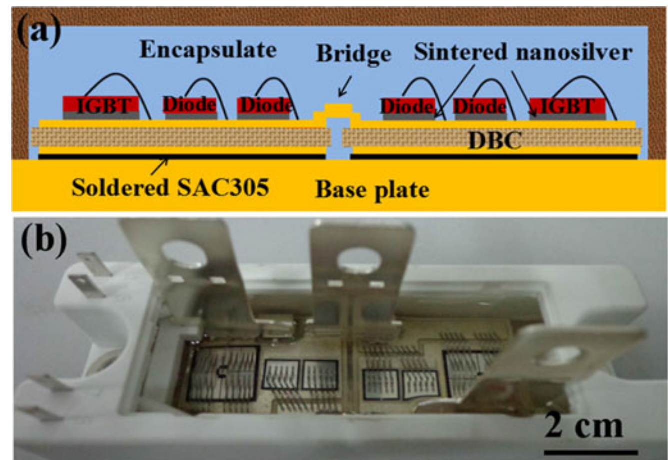

Fig. 3. (a) Cross-sectional sketch and (b) typical image of a multichip phase-leg IGBT module using the pressureless sintered nanosilver.

in the pressureless sintered nanosilver, i.e., less than 2%. It is important to eliminate the voids in die attachment because the voids impact the service lifetime of power modules greatly. The voids could be accumulated and grown larger and larger by thermomechanical stress, which could increase thermal resistance resulting in greater temperature fluctuations within the power module [36]. This excess heat accumulation may accelerate further degradation of the power devices.

B. Package Structure

A typical image of an as-fabricated multichip phase-leg 1200-V/150-A IGBT module using the pressureless sintered nanosilver was shown in Fig. 3 schematically. The module includes two identical patterned DBC substrates joined with a copper base plate. The DBC substrates were used to provide a current loop from the bus bar to the chip and then back, dissipate the generated heat by the power loss of the power devices, and isolate the electrical terminals from each other [37]. The copper sheets of the DBC substrates were metallized with a 0.5-μm-thick silver film. One IGBT chip (12.56 mm $\times$ 12.56 mm) and two diode chips (6.3 mm $\times$ 6.3 mm) were attached on each DBC substrate by pressureless sintering of nanosilver paste as one semibridge element. Each power module consists of the two elements. The terminals and the bridges were connected with the DBC substrates by reflowing SAC305 solder. The bridge was used to connect the two parallel DBC substrates. Sylgard 527 [38] was used as an encapsulant (see the blue part in Fig. 3(a)) due to its relatively good thermal properties and high-temperature stability. Finally, the encapsulant was cured at 150 °C for 30 min.

III. Reliability Tests

In order to evaluate the reliability of this multichip phase-leg IGBT modules using the pressureless sintered nanosilver, both second-level and minute-level power cycling tests were used here. In addition, the high-temperature solder, i.e., Sn5Pb92.5Ag2.5, was used as a contrast die-attach material to assess the feasibility of the die attachment by pressureless sintering of nanosilver paste.

A. Active Power Cycling

Fig. 4(a) shows the schematic circuit diagram of the test bench for power cycling tests. For each power cycling test, i.e., second-level or minute-level power cycling test, five IGBT modules using sintering of nanosilver paste were connected in series, while five IGBT modules using the Sn5Pb92.5Ag2.5 solder were connected in the other series. A total of 20 IGBT modules were tested in this study. The DUT_A and DUT_B were used as the standard IGBT modules to control the switch

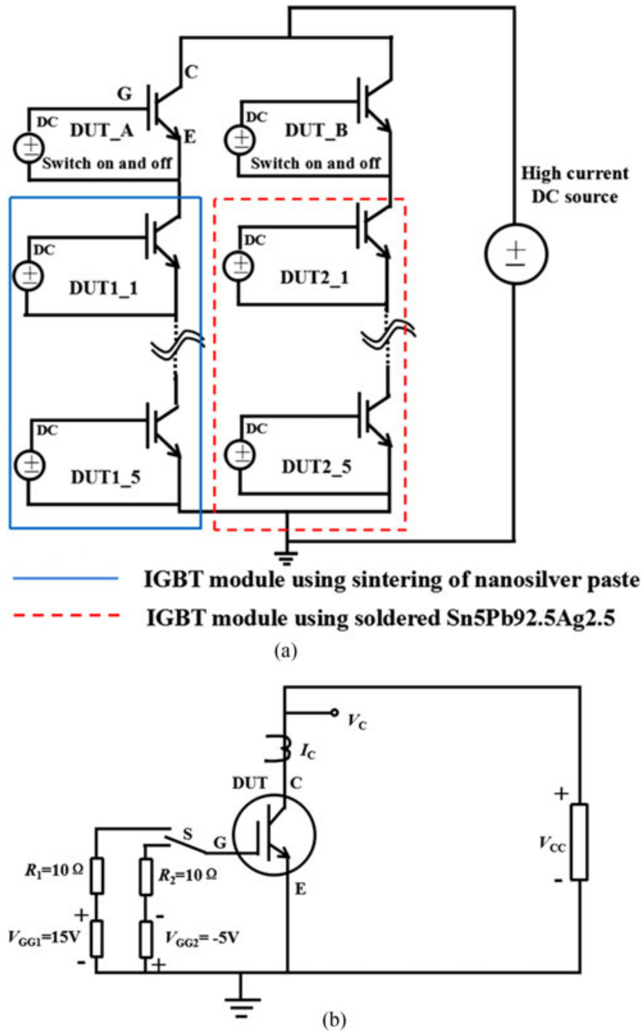

Fig. 4. (a) Schematic circuit diagram of the test bench for power cycling tests and (b) circuit design for aging each single IGBT module.

on and off during the power cycling tests. Each IGBT module was considered as a single element, which was aged by the power cycling test according to the circuit as shown in Fig. 4(b). The V_{GE} was set to $+15$ and -5 V during the power on and off, respectively. For the second-level power cycling test, the fixed current is about 150 A and the power is 270–300 W. The fixed on and off time are both 5 s. For the minute-level power cycling test, the fixed current is about 60 A and the power is 100–120 W. The fixed on and off time are 2 and 4 min, respectively. Failure criteria was defined as 20% increase in collector–emitter saturation voltage ($V_{\mathrm{CE(sat)}}$) in the power cycling test [39].

The junction temperature (T_j) was measured by means of a temperature sensitive electrical parameter [40]–[42]. The value of T_j could be calculated by

$$T_j = T_c + \frac{V_{\mathrm{CE}_j} - V_{\mathrm{CE}_c}}{K} \tag{1}$$

where T_c is the case temperature, which was directly measured by thermocouple. V_{CE_j} and V_{CE_c} are the collector–emitter voltage at junction temperature and case temperature, respectively. K is the factor connecting the temperature sensitive

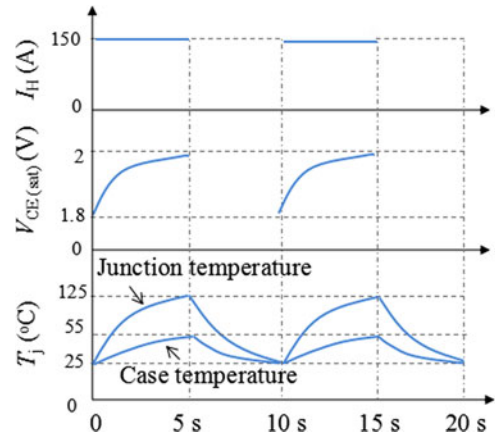

Fig. 5. Profile of second-level power cycling test.

parameter to the p-n junction temperature [43]. Since the collector–emitter voltage varies linearly with the temperature of the IGBT device, the *K*-factor could be calculated from the absolute slope of the line and the value is 9.5 mV/°C in this case. Although there is a certain difference in the *K* factor of different IGBT chips, we have screened the IGBT chips by measuring V_{CE} of all the IGBTs to guarantee that the *K* value of each chip is almost the same as 9.5 mV/°C before the module fabrication. Therefore, we assumed the *K* factor of all the IGBT herein as 9.5 mV/°C in order to simplify the *K* factor measurement.

B. Second-Level Power Cycling Test

The objective of this test is to demonstrate the effect of die-attach materials on the reliability of wire bonding. Fig. 5 shows the profile of the power cycling test. The period of each power cycles is only 10 s, i.e., 5 s for power on and 5 s for power off. The junction temperature swings between 25 and 125 °C, whereas case temperature varies between 25 and 55 °C.

Generally, both Au and Al can be used as wirebond materials of power modules. Considering the cost, we selected Al wires as the wirebond material in this study. Al wires with 15 mil diameter were used for the 1200-V/150-A IGBT modules. It is also worth noting that the bonding between Al wires and Al metallization on the backside of the IGBT chips is not susceptible to the Kirkendall voids so that the Al wire is more reliable than the Au one for bonding Al metallization [44]. Before the wirebond, plasma cleaning was used to remove thin layers of the oxides and the organic residues.

As we may know, the wirebond quality is mainly dependent on ultrasonic power, bonding force, and bonding time. The ultrasonic power was herein set as 1.0–1.6 W. If the power for breaking through the initial oxides is too high, die cratering may be present. However, bond "nonstick" type failures may also occur by reducing the power [45]. The bonding force was set in the range of 600–800 gf. A too high magnitude could damage the bond pad metallization or the pad structure underneath cratering, while too low-force magnitude might lift ball bond due to ineffective transducer power transmitted through the smashed ball [46]. The bonding time was set in the range of 100–150 ms. Excessive bonding time can increase tool

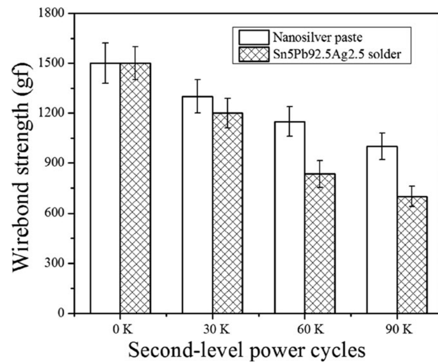

Fig. 6. Comparison of the wirebond strength before and after second-level power cycles.

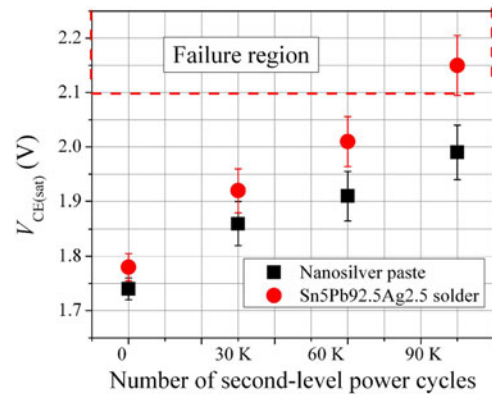

Fig. 7. $V_{\mathrm{CE(sat)}}$ of the two kinds of IGBT modules versus number of second-level power cycles.

maintenance due to contamination build up and wear, and damage or burn appearing wirebonds in areas where the tool contacts the bond [47].

Fig. 6 shows the comparison of wirebond strength between the module with nanosilver paste and the one with Sn5Pb92.5Ag2.5 solder before and after several power cycles. The two kinds of as-prepared power modules show the same wirebond strength. However, the wirebond strength of the module with Sn5Pb92.5Ag2.5 solder decreases sharply after power cycles. The strength of the power module with nanosilver paste solder is even 38% higher than the one with Sn5Pb92.5Ag2.5 after 60 000 cycles. The reason for this phenomenon may be attributed to the difference of the die-attach material. The sintered silver has a high thermal conductivity of 240 W/m·K [48], while the soldered Sn5Pb92.5Ag2.5 is only about 44 W/mK. For the sintered device, it allowed an improved heat transfer through the die attachment out of the package. The solder, however, is susceptible to delamination or voids in the long service, which may cause local overheating and lead to the increase of the junction temperature [49]. High temperature developed in emitter wires and in wirebond joints causes wire melting and lifting failures [50], resulting in the strength reduction of the wirebonds. On the other hand, the degradation of the solder die attachment results in a local high-temperature swing (ΔT), which is higher than that of the sintered device [51]. The different ΔT had also been confirmed by Krebs *et al.* [52] who had compared the reliability of CucorAl wirebonds between soldered devices and sintered devices. In their study, at the beginning of the power cycling test, the current was adjusted to get a $\Delta T = 110$ K. After 50 000 power cycles, the ΔT of the soldered device increased to 132 K, while the sintered device increased only to 116 K. High ΔT is easier to cause the Al wirebond to bear greater compressive or tensile stresses because of the mismatch of their CTE [53]. During the power cycling tests, the Al wirebond constantly endures the temperature swings during the operation between silicon chips and aluminum wires. As a result, the stresses could destroy the Al wirebonds of the IGBT module potentially in the forms of cracking and creep, which lead to the strength reduction of the wirebonds.

It can be indicated that the wire-lifting failure is easier to be present in the power module with Sn5Pb92.5Ag2.5 solder. The failure is attributed to the physical changes of the Al wire because of cyclic thermomechanical stress which could result cracks near the heel and toe of the Al wire [54]. Once some of Al wires fail, the remaining wires have to conduct more current, resulting in a current redistribution in the chip and an increase of the average junction temperature, which could also accelerate the degradation of the failure in the remaining Al wires. Therefore, the stable thermal properties of the die-attach material, i.e., nanosilver paste, result in a longer lifetime of the Al wire bond and, consequently, in a longer lifetime of the power electronic devices.

Fig. 7 shows the typical IGBT $V_{\mathrm{CE(sat)}}$ versus the number of power cycles between the modules with nanosilver paste and the one with Sn5Pb92.5Ag2.5 solder. The $V_{\mathrm{CE(sat)}}$ was tested in a static condition, which means that the power cycle test is interrupted for the measurement. The beauty of this method is that the current for static $V_{\mathrm{CE(sat)}}$ measurement is the rated current of the power module with very good accuracy [55]. After 60 000 power cycles, the $V_{\mathrm{CE(sat)}}$ of the IGBT module with Sn5Pb92.5Ag2.5 solder increases to 2.01 V, which is 0.11 V higher than that with nanosilver paste. This may be due to the crack propagation in the Al wire bonds and subsequent bonds lift off [56]. The increased $V_{\mathrm{CE(sat)}}$ should cause additional power loss, leading to a temperature rise of the entire IGBT module. The modules with Sn5Pb92.5Ag2.5 solder were failed after 60 000 power cycles, which is earlier than the ones with nanosilver paste consequently. The modules with nanosilver paste show longer lifetime for the second-level power cycling and failed after at least 90 000 cycles.

C. Minute-Level Power Cycling Test

The reliability of die attachment is as important as that of wirebonds. A good die attachment must have to meet the desired functionality that could affect mechanical, thermal, and electrical properties of power modules. To evaluate the reliability of die attachment in the multichip IGBT modules, a minute-level power cycling test was performed and its profile is shown in Fig. 8. Each power cycle lasts 6 min so that there is enough time for the heat to dissipate from power chip to die attachment. The

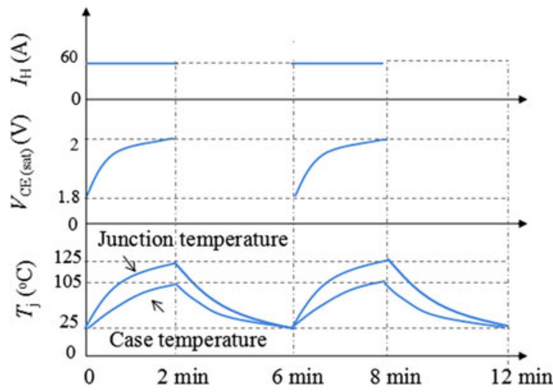

Fig. 8. Schematic for the minute-level power cycling setup.

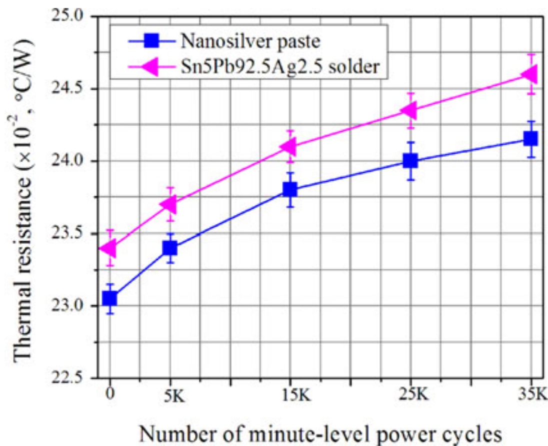

Fig. 9. Thermal resistance of two kinds of IGBT modules with different die-attach materials versus number of minute-level power cycles.

junction temperature swings between 25 and 125 °C, whereas the case temperature varies between 25 and 105 °C.

Fig. 9 shows the comparison of the thermal resistance between the IGBT module with pressureless sintered nanosilver and the one with soldered Sn5Pb92.5Ag2.5. The thermal resistance of the IGBT module can be defined as the temperature drop between junction temperature T_j and case temperature T_c divided by the power loss P [57]

$$R_{\text{th}} = \frac{T_j - T_c}{P}. \tag{2}$$

The thermal resistance increases with increase in the number of power cycles. Before power cycling, the thermal resistance of the commercial IGBT module with soldered Sn5Pb92.5Ag2.5 is $0.234\,^{\circ}\text{C/W}$, which is 1.5% higher than that of our as-prepared IGBT module with pressureless sintered nanosilver. After 35 000 minute-level power cycles, the resistance of the IGBT module with soldered Sn5Pb92.5Ag2.5 increased to $0.246\,^{\circ}\text{C/W}$, which is 2.1% higher than that of the IGBT module with the pressureless sintered nanosilver. It was indicated that the solder layer could deteriorate the capability of heat dissipation during the minute-level power cycles. The junction temperature of the IGBT module with the soldered Sn5Pb92.5Ag2.5 is higher than the one with the pressureless sintered nanosilver. As a result, the Si p-i-n diode reverse-recovery current increased substantially in the case of higher junction temperature because of the increase of the lifetime of the carrier at the higher temperatures [58]. The reverse-recovery current also induces extra reverse-recovery losses of the Si p-i-n diode when the device is turned off, leading to accelerate degradation of the power module with soldered Sn5Pb92.5Ag2.5 [59]. It is worth noting that the evaluated temperature may have no effect on the reverse-recovery loss of SiC Schottky diodes because they are unipolar devices proposed to have a negligible reverse-recovery current during turn off [60]. It is also worth noting that the difference in the overall thermal resistance of the IGBT modules module with pressureless sintered nanosilver and the one with soldered Sn5Pb92.5Ag2.5 is not significant. It may be that the thermal resistance of die attachment is only a small fraction of the overall thermal resistance, and the benefit brought by the pressureless sintered nanosilver becomes less significant.

Although the difference of the thermal resistance between the two modules is not significant, the use of nanosilver paste as a die-attach material is more important for further applications, especially in the high-temperature environment. For the IGBT module with soldered Sn5Pb92.5Ag2.5, there is a standard two-solder reflow process; the melting point of solder using as die attachment should be higher than that of one using to bond DBC substrate with base plate. Therefore, the Sn5Pb92.5Ag2.5 is used as a die attachment and the Sn96.5Ag3.0Cu0.5 is selected for bonding DBC substrate with base plate. However, the Sn96.5Ag3.0Cu0.5 with the low melting point is more susceptible to creep failure compared with other die-attach materials with the higher melting point in the long-term service. Since the melting point of the sintered nanosilver is as high as 961 °C, many other bonding materials with high melting point could be selected for bonding DBC substrate and base plate. In addition, we also try to use nanosilver paste as DBC-attach layer in our further work so as to obtain better long-term reliability.

Any void, crack, and delamination in the die attachment could also increase the thermal resistance considerably because the thermal conductivity of air is extremely lower than that of any bulk metal [61]. Although the void ratio of the two kinds of die-attach layers was both acceptable for the industrial electronics, the void of sintered silver joints was small and round in shape, while the void of soldered Sn5Pb92.5Ag2.5 joints was irregular in shape. In the case of cyclic loading, the stresses are evenly distributed around the round void, while the stresses are easy to gather at the tip of irregular void. The uneven distribution of stress may promote the initiation and growth of cracks easily. On the other hand, the intermetallic compounds (IMCs) could be generated in the soldered Sn5Pb92.5Ag2.5 joints, whereas no IMC could be formed in the sintered joints, which are made up of metallic silver. These IMCs are generally more brittle than the base metal and have a negative impact on the reliability of soldered Sn5Pb92.5Ag2.5 joint and the IMCs can easily lead to crack initiation and accelerate the propagation of fatigue cracks, and eventually promote the accumulation of damage [61]. As a result, the thermal resistance of the module with soldered Sn5Pb92.5Ag2.5 increases faster than the one with sintered nanosilver during the minute-level power cycles.

During each power cycle, considerable temperature gradients are generated inside the IGBT module. Thermomechanical

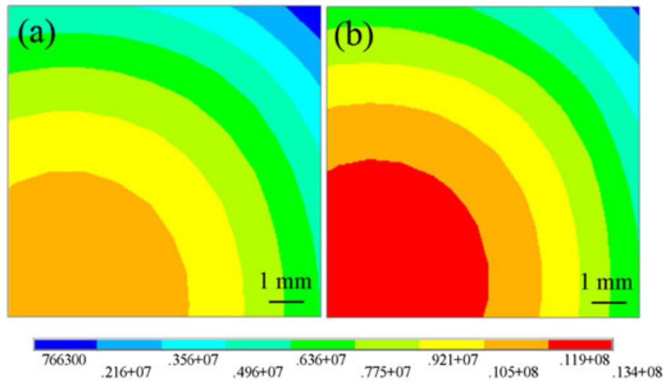

Fig. 10. Von-Mises stress distribution of die attachment of (a) pressureless sintered nanosilver and (b) soldered Sn5Pb92.5Ag2.5.

stresses are also easily produced in the die-attach layers due to the temperature fluctuations. A finite-element modeling was used to simulate and compare the thermomechanical stress distribution between sintered nanosilver and soldered Sn5Pb92.5Ag2.5. Fig. 10 shows the von-Mises stress distribution of the die-attach layer at the end of the fifth power cycle. As seen, the maximum stresses of both die-attach layers are easily located along the center of the layers. The maximum von-Mises stress of the soldered Sn5Pb92.5Ag2.5 layer is 13.4 MPa, which is 2.9 MPa higher than that of the sintered nanosilver layer. Large thermomechanical stresses can destroy the bonding layers, especially for the interface between the soldered Sn5Pb92.5Ag2.5 and substrate. It is well known that the cyclic thermomechanical stress plays an important role in the mechanism of void formation [62]. The induced microcracks at the interface between the bonding layer and substrate may cause faster and more extensive laminate cracking during the thermal cycles.

Fig. 11 shows the comparison of *I–V* characteristics at different number of power cycles between the module with pressureless sintered nanosilver and the one with soldered Sn5Pb92.5Ag2.5. The *I–V* curves of these IGBT modules were measured by a static testing system (CREA, STD MT100s-20). The on-state resistance increases with increase in the number of power cycles. The forward characteristics of both IGBTs and diodes were recorded with respect to the different temperatures. Since the relationship between the on-state current and voltage is fairly linear [63]. Therefore, the on-state resistance can be expressed as follows:

$$R_{\rm CE} = (V_{\rm CE} - V_t)/I_C \quad (3)$$

$$R_F = (V_F - V_f)/I_F \quad (4)$$

where $R_{\rm CE}$ and R_F represent the on-state resistances of IGBT and diode, respectively, while V_t and V_f represent the built-in voltages of the IGBT and the diode, respectively. The on-state resistance of the IGBT of the module using sintered nanosilver was 9% lower than that using soldered Sn5Pb92.5Ag2.5 after 35 000 power cycles. The on-state resistance of the diode of the module using sintered nanosilver was 6% lower than that using soldered Sn5Pb92.5Ag2.5 after 35 000 power cycles. The on-state resistance includes three parts: the on-resistance of the power chip, the on-resistance of the wirebond, and the on-resistance of the die attachment. Because the power chips used in the two kinds of IGBT modules could be treated as identical as each other, the increased on-resistance may mainly depend on not only the degradation of die attachment but also the wirebond heel crack or failure.

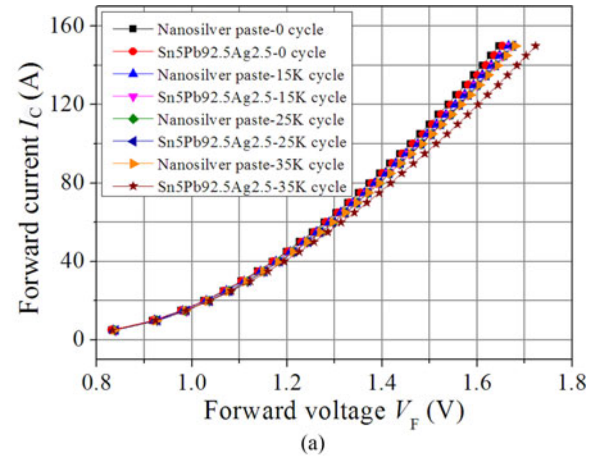

(a)

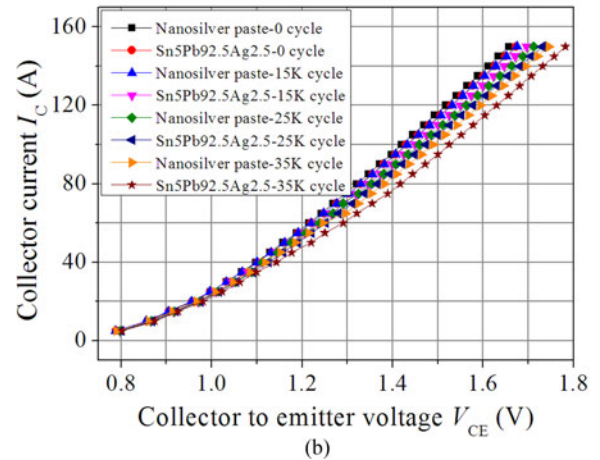

(b)

Fig. 11. Forward characteristics at different minute-level power cycles. (a) Diode (b) IGBT.

Compared to the sintered device, the soldered device is more prone to cracks and creep degradation in the wirebonds because of the low thermal conductivity and the possible formation of IMCs for the solders [64]. The formation of cracks and creep degradation could lead to an increase in the on-resistance of the wirebonds, resulting in the decrease of capability of taking current in the local hotspot/crack region. Current imbalance could occur among the wires because the rest wires in the other area without hotspot/cracks have to take more current through the power device. Consequently, more heat could be generated further in these wirebonds and may cause wire melting and lifting failures, which also promotes the increase of on-resistance of the wirebonds.

For the die attachment, the resistance of the die attachment can be calculated as

$$R = \rho \frac{L}{S} \quad (5)$$

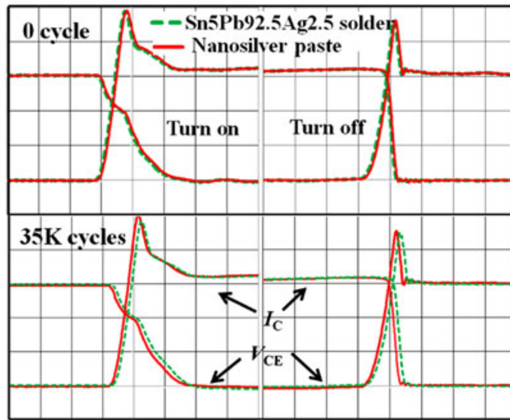

Fig. 12. Switching waveforms of the IGBT modules before and after 35-K power cycles.

where ρ, L, and S are the resistivity, the length, and the cross-sectional area of the die attachment, respectively. The crack growth was likely to be interrupted by the uniformly distributed pores in the sintered silver joints [65]. Therefore, few cracks could be present in the sintered nanosilver. On the contrary, the cracks are easier to be generated in the soldered Sn5Pb92.5Ag2.5 joints due to irregular voids and IMCs [66]. The more cracks in the die attachment, the smaller the cross-sectional area (S) of the die attachment. Therefore, the on-state resistance also increases with the increase in the number of cycles because of the increase of the cracks in the die attachment.

The switching characteristics were also compared between the two kinds of IGBT modules before and after the minute-level power cycling test. The test temperature was fixed at 25 °C. The switching behavior of the devices was measured by the double-pulse testing method [67]. The test conditions included dc bus voltage $V_{CC} = 600$ V, current $I_C = 150$ A, gate resistance $R_G = 15\,\Omega$, and load inductance $L = 200\,\mu$H.

The switching waveforms and switching characteristics of the two IGBT modules were shown in Figs. 12 and 13, respectively. Before the power cycles, the switching waveforms of the IGBT module using pressureless sintered nanosilver match well with those of the commercial IGBT module using soldered Sn5Pb92.5Ag2.5. The total switching loss of these two IGBT modules was about 42.5 mJ. After 35 000 power cycles, the total switching loss of the IGBT module with soldered Sn5Pb92.5Ag2.5 was measured to be 56.5 mJ. However, the IGBT module with sintered nanosilver is only 48.9 mJ. Large switching losses not only degrade conversion efficiency but may also lead to the need to take away more heat generated in the device and driver circuitry [68]. The maximum junction temperature of the IGBT module with soldered Sn5Pb92.5Ag2.5 should be higher than that of the IGBT module with pressureless sintered nanosilver in the same conditions because of the higher power loss and the lower thermal conductivity. As a result, the Si p-i-n diode reverse-recovery current as well as reverse recovery energy has to increase over a long duration, resulting in current overshoot and extra turn-on losses of the complimentary IGBTs [69].

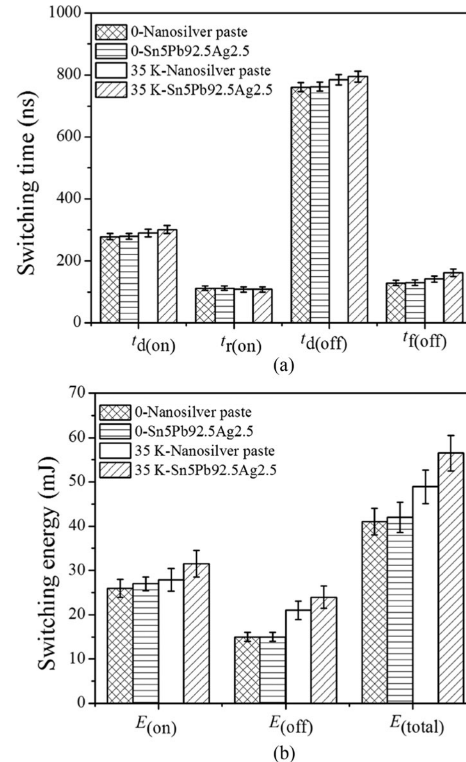

Fig. 13. Switching characteristics of the IGBT modules before and after 35-K power cycles.

IV. Conclusion

This paper presents the reliability of a multichip phase-leg IGBT module bonded by pressureless sintering of nanosilver paste considering power cycling test. By second-level power cycling test (junction temperature: 25 to 125 °C, case temperature: 25 to 55 °C), the lifetime of the IGBT module with soldered Sn5Pb92.5Ag2.5 was 30 000 cycles lower than the one with pressureless sintered nanosilver. After 35 000 minute-level power cycling test (junction temperature: 25 to 125 °C, case temperature: 25 to 105 °C), the thermal resistance, on-state resistance, and total switching energy of the IGBT module using pressureless sintered nanosilver were 2.1%, 9.0%, and 13.4% lower than that of commercial one, respectively. In summary, this study presents a efficient way different from existing ones to optimize the large-area die attachment for power electronic packaging, especially high-temperature applications, e.g., for assembling SiC or GaN devices at high temperature.

References

[1] U. M. Choi, K. B. Lee, and F. Blaabjerg, “Study and handling method of power IGBT module failure in power electronic converter system,” *IEEE Trans. Power Electron.*, vol. 30, no. 5, pp. 2517–2533, Dec. 2015.

[2] K. J. Li, G. Y. Tian, L. Cheng, A. J. Yin, W. P. Cao, and S. Crichton, “State detection of bond wires in IGBT modules using eddy current pulsed thermography,” *IEEE Trans. Power Electron.*, vol. 29, no. 9, pp. 5000–5009, Apr. 2014.

[3] A. Bryant *et al.*, “Investigation into IGBT dv/dt during turn-off and its temperature dependence,” *IEEE Trans. Power Electron.*, vol. 26, no. 10, pp. 3019–3031, Oct. 2011.

[4] S. N. Li, L. M. Tolbert, F. Wang, and F. Z. Peng, "P-cell and N-cell based IGBT module: Layout design, parasitic extraction, and experimental verification," in *Proc. Appl. Power Electron. Conf.*, Fort Worth, TX, USA, Mar. 2011, pp. 372–378.

[5] H. Mirzaee, A. De, A. Tripathi, and S. Bhattacharya, "Design comparison of high-power medium-voltage converters based on a 6.5-kV Si-IGBT/Si-PiN diode, a 6.5-kV Si-IGBT/SiC-JBS diode, and a 10-kV SiC-MOSFET/SiC-JBS diode," *IEEE Trans. Ind. Appl.*, vol. 50, no. 4, pp. 2728–2740, Jul. 2014.

[6] A. Hensler, J. Lutz, M. Thoben, and K. Guth, "First power cycling results of improved packaging technologies for hybrid electrical vehicle applications," in *Proc. Int. Conf. Integr. Power Electron. Syst.*, Nuremberg, Germany, Mar. 2010, pp. 1–5.

[7] S. C. Fu, Y. H. Mei, G. Q. Lu, X. Li, G. Chen, and X Chen, "Pressureless sintering of nanosilver paste at low temperature to join large area (≥100 mm^2) power chips for electronic packaging," *Mater. Lett.*, vol. 128, no. 1, pp. 42–45, Aug. 2014.

[8] M. Y. Tsai, C. H. J. Hsu, and C. T. O. Wang, "Investigation of thermomechanical behaviors of flip chip BGA packages during manufacturing process and thermal cycling," *IEEE Trans. Compon. Packag. Technol.*, vol. 27, no. 3, pp. 568–576, Sep. 2004.

[9] J. H. L. Pang, D. Y. R. Chong, and T. H. Low, "Thermal cycling analysis of flip-chip solder joint reliability," *IEEE Trans. Compon. Packag. Technol.*, vol. 24, no. 4, pp. 705–712, Aug. 2001.

[10] B. Ji, X. G. Song, E. Sciberras, W. P. Cao, Y. H. Hu, and V Pickert, "Multiobjective design optimization of IGBT power modules considering power cycling and thermal cycling," *IEEE Trans. Power Electron.*, vol. 306, no. 5, pp. 2493–2504, Dec. 2014.

[11] E. Özkol, F. Brem, C. L. Liu, S. Hartmann, and A. Kopta, "Enhanced power cycling performance of IGBT modules with a reinforced emitter contact," *Microelectron. Rel.*, vol. 55, no. 6, pp. 912–918, May 2015.

[12] S. Kim, K. S. Kim, G. Izuta, and K. Suganuma, "Reliability of die attached AlN-DBC module using Zn-Sn high temperature lead-free solders," in *Proc. Electron. Syst. Integr. Technol. Conf.*, Greenwich, U.K., Sep. 2008, pp. 1–4.

[13] P. Yang, D. J. Liu, Y. F. Zhao, Y. Q. Tang, and H. Wang, "Approach on the life-prediction of solder joint for electronic packaging under combined loading," *IEEE Trans. Rel.*, vol. 62, no. 4, pp. 870–875, Dec. 2013.

[14] B. Ji *et al.*, "In situ diagnostics and prognostics of solder fatigue in IGBT modules for electric vehicle drives," *IEEE Trans. Power Electron.*, vol. 30, no. 3, pp. 1535–1543, Mar. 2015.

[15] D. W. Xiang, L. Ran, P. Tavner, S. Y. Yang, A. Bryant, and P. Mawby, "Condition monitoring power module solder fatigue using inverter harmonic identification," *IEEE Trans. Power Electron.*, vol. 27, no. 1, pp. 235–247, Jan. 2012.

[16] S. W. Yoon, M. D. Glover, and K. Shiozaki, "Nickel-Tin transient liquid phase bonding toward high-temperature operational power electronics in electrified vehicles," *IEEE Trans. Power Electron.*, vol. 306, no. 5, pp. 2493–2504, Dec. 2014.

[17] Y. Zhai, T. H. North, and J. S. Rodrigues, "Transient liquid-phase bonding of alumina and metal matrix composite base materials," *J. Mater. Sci.*, vol. 32, no. 6, pp. 1393–1397, Mar. 1997.

[18] H. Yu and D. Shangguan, "Solidification and reliability of lead-free solder interconnection," *Soldering Surf. Mount Technol.*, vol. 25, no. 1, pp. 31–38, Feb. 2013.

[19] G. Chen, L Yu, Y. H. Mei, X. Li, X. Chen, and G. Q. Lu, "Uniaxial ratcheting behavior of sintered nanosilver joint for electronic packaging," *Mater. Sci. Eng. A*, vol. 591, no. 1, pp. 121–129, Jan. 2014.

[20] X. Chen, R. Li, K. Qi, and G. Q. Lu, "Tensile behaviors and ratcheting effects of partially sintered chip-attachment films of a nanoscale silver paste," *J. Electron. Mater.*, vol. 37, no. 10, pp. 1574–1579, Oct. 2008.

[21] P. Rajaguru, H. Lu, and C Bailey, "Sintered silver finite element modelling and reliability based design optimisation in power electronic module," *Microelectron. Rel.*, vol. 55, no. 6, pp. 919–930, May 2015.

[22] X. Li, X. Chen, and G. Q. Lu, "Isothermal low cycle fatigue behavior of nano-silver sintered single lap shear joint," in *Proc. Int. Conf. Electron. Packag. Technol. High Density Packag.*, Guilin, China, Aug. 2012, pp. 13–16.

[23] G. Chen, L. Yu, Y. H. Mei, X. Li, X Chen, and G. Q. Lu, "Reliability comparison between SAC305 joint and sintered nanosilver joint at high temperatures for power electronic packaging," *J. Mater. Process. Technol.*, vol. 214, no. 9, pp. 1900–1908, Sep. 2014.

[24] C. Weber, M. Hutter, C. Ehrhardt, and K. D. Lang, "Failure analysis of Ag sintered joints after power cycling under harsh temperature conditions from 30 °C up to 180 °C," in *Proc. Eur. Microelectron. Packag. Conf.*, Friedrichshafen, Germany, Sep. 2015, pp. 14–16.

[25] C. Weber, M. Hutter, S. Schmitz, and K. D. Lang, "Dependency of the porosity and the layer thickness on the reliability of Ag sintered joints during active power cycling," in *Proc. Electron. Compon. Technol. Conf.*, May 2015, pp. 26–29.

[26] K. Osonoe, T. Asai, M. Aoki, H. Kida, and N. Nakano, "Comparison of thermal stress concentration and profile between power cycling test and thermal cycling test for power device heat dissipation structures using Ag sintering chip-attachment," in *Proc. Int. Conf. Electron. Packag.*, Hokkaido, Japan, Apr. 2016, pp. 631–634.

[27] F. L. Henaff, S. Azzopardi, J. Y. Deletage, E. Woirgard, S. Bontemps, and J. Joguet, "A preliminary study on the thermal and mechanical performances of sintered nano-scale silver die-attach technology depending on the substrate metallization," *Microelectron. Rel.*, vol. 52, nos. 9/10, pp. 2321–2325, Sep. 2012.

[28] L. Jiang, G. Y. Lei, K. D. T. Ngo, G. Q. Lu, and S. F. Luo, "Evaluation of thermal cycling Reliability of sintered nanosilver versus soldered joints by curvature measurement," *IEEE Trans. Compon., Packag., Manuf. Technol.*, vol. 4, no. 5, pp. 751–761, May 2014.

[29] M. Knoerr, S. Kraft, and A. Schletz, "Reliability assessment of sintered nanosilver die attachment for power semiconductors," in *Proc. Electron. Packag. Technol. Conf.*, Singapore, Dec. 2010, pp. 56–61.

[30] Y. H. Mei, T. Wang, X. Cao, G. Chen, G. Q. Lu, and X. Chen, "Transient thermal impedance measurements on low-temperature-sintered nanoscale silver joints," *J. Electron. Mater.*, vol. 41, no. 11, pp. 3152–3160, Nov. 2012.

[31] C. Göbl and J. Faltenbacher, "Low temperature sinter technology die attachment for power electronic applications," in *Proc. Int. Conf. Integr. Power Electron. Syst.*, Nuremberg, Germany, Mar. 2010, pp. 16–18.

[32] T. Stockmeier, P. Beckedahl, C. Göbl, and T. Malzer, "SKiN: Double side sintering technology for new packages," in *Proc. Int. Symp. Power Semicond. Devices*, May 2011, pp. 23–26.

[33] X. Cao, T. Wang, K. D. Ngo, and G. Q. Lu, "Characterization of lead-free solder and sintered nano-silver die-attach layers using thermal impedance," *IEEE Trans. Compon., Packag., Manuf. Technol.*, vol. 1, no. 4, pp. 495–501, Apr. 2012.

[34] H. G. Zheng, K. D. T. Ngo, and G. Q. Lu, "Temperature cycling reliability assessment of die attachment on bare copper by pressureless nanosilver sintering," *IEEE Trans. Device Mater. Rel.*, vol. 15, no. 2, pp. 214–219, Jun. 2015.

[35] F. Dugal and M. Cippa, "Study of thermal cycling and temperature aging on PbSnAg die attach solder joints for high power modules," *Microelectron. Rel.*, vol. 54, no. 9, pp. 1856–1861, Sep. 2014.

[36] D. C. Katsis and J. D. V. Wyk, "Void-induced thermal impedance in power semiconductor modules: Some transient temperature effects," *IEEE Trans. Ind. Electron.*, vol. 39, no. 5, pp. 1239–1246, Sep. 2003.

[37] L. Kamenova, Y. Avenas, C. Schaeffer, S. Tzanova, G. Kapelski, and S. H. Juergen, "DBC technology for extremely thin flat heat pipes," *IEEE Trans. Ind. Electron.*, vol. 45, no. 5, pp. 1763–1769, Sep. 2009.

[38] Dow Corning(R), Sylgard 527 silicone dielectric Gel product information, 2008.

[39] V. A. Sankaran, C. Chen, C. S. Avant, and X. Xu, "Power cycling reliability of IGBT power modules," in *Proc. IEEE Ind. Appl. Soc. 32nd Annu. Meet. Conf.*, New Orleans, LA, USA, Oct. 1997, pp. 5–9.

[40] R. Schmidt and U. Scheuermann, "Using the chip as a temperature sensor—The influence of steep lateral temperature gradients on the Vce(T)-measurement," in *Proc. Eur. Conf. Power Electron. Appl.*, Barcelona, Spain, Sep. 2009, pp. 8–10.

[41] P. Ghimire, A. R. D. Vega, S. Beczkowsk, S. Munk-Nielsen, B. Rannested, and P. B. Thogersen, "An online Vce measurement and temperature estimation method for high power IGBT module in normal PWM operation," in *Proc. Int. Power Electron. Conf.* Hiroshima, Japan, May 2014, pp. 18–21.

[42] M. Held, P. Jacob, G. Nicoletti, P. Scacco, and M. H. Poech, "Fast power cycling test for IGBT modules in traction application," in *Proc. Int. Conf. Power Electron. Drive Syst.*, Singapore, May 1997, pp. 26–29.

[43] G. Chen *et al.*, "Transient thermal performance of IGBT power modules attached by low-temperature sintered nanosilve," *IEEE Trans. Device Mater. Rel.*, vol. 12, no. 1, pp. 124–132, Mar. 2012.

[44] S. Murali, N. Srikanth, and C. J. Vath III, "Effect of wire size on the formation of intermetallics and Kirkendall voids on thermal aging of thermosonic wire bonds," *Mater. Lett.*, vol. 58, no. 25, pp. 3096–3101, Oct. 2004.

[45] L. T. Nguyen, D. McDonald, and A. R. Danker, "Optimization of copper wire bonding on A1-Cu metallization," *IEEE Trans. Compon., Packag., Manuf. Technol. A*, vol. 18, no. 2, pp. 423–429, Jan. 1995.

[46] L. C. Chia, C. K. Yau, and T. S. Chee, "Effect of impact force towards Cu wire bonding reliability," in *Proc. Electron. Packag. Technol. Conf.*, Singapore, Dec. 2015, pp. 2–4.

[47] D. T. Rooney, D. P. Nager, D. Geiger, and D Shanguan, "Evaluation of wire bonding performance, process conditions, and metallurgical integrity of chip on board wire bonds," *Microelectron. Rel.*, vol. 45, no. 2, pp. 379–390, Jan. 2005.

[48] H. D. Yan, Y. H. Mei, X. Li, P. Zhang, and G. Q. Lu, "Degradation of high power single emitter laser modules using nanosilver paste in continuous pulse conditions," *Microelectron. Rel.*, vol. 55, no. 12, pp. 2532–2541, Dec. 2015.

[49] W. C. Wu, M. Held, P. Jacob, P. Scacco, and A. Birolini, "Investigation on the long term reliability of power IGBT modules," in *Proc. Int. Symp. Power Semicond. Devices*, Yokohama, Japan, May 1995, pp. 23–25.

[50] W. Wu *et al.*, "Thermal reliability of power insulated gate bipolar transistor (IGBT) modules," in *Proc. Semicond. Thermal Meas. Manage. Symp.*, Austin, TX, USA, Mar. 1996, pp. 5–7.

[51] P. Q. Ning, G. Y. Lei, F.Wang, G. Q. Lu, K. D. T. Ngo, and K. Rajashekara, "A novel high-temperature planar package for SiC multichip phase-leg power module," *IEEE Trans. Power Electron.*, vol. 25, no. 8, pp. 2059–2067, Aug. 2010.

[52] T. Krebs, S. Duch, W. Schmitt, S. Kötter, P. Prenosil, and S. Thomas, "A breakthrough in power electronics reliability-New die attach and wire bonding materials," in *Proc. Electron. Compon. Technol. Conf.*, Las Vegas, NV, USA, May 2013, pp. 28–31.

[53] K. Dai and L Shaw, "Thermal and stress modeling of multi-material laser processing," *Acta Mater.*, vol. 49, no. 20, pp. 4171–4181, Dec. 2001.

[54] J. Onuki, M. Koizumi, and M. Suwa, "Reliability of thick Al wire bonds in IGBT modules for traction motor drives," *IEEE Trans. Adv. Packag.*, vol. 23, no. 1, pp. 108–112, Feb. 2000.

[55] B. Gehman, "Bonding wire microelectronic interconnections," *IEEE Trans. Compon., Hybrids, Manuf. Technol.*, vol. 3, no. 3, pp. 375–383, Sep. 1980.

[56] S. Mazzei, M. Madia, S. Beretta, A. Mancaleoni, and S. Aparo, "Analysis of Cu-wire pull and shear test failure modes under ageing cycles and finite element modelling of Si-crack propagation," *Microelectron. Rel.*, vol. 54, no. 11, pp. 2501–2512, Nov. 2014.

[57] M. Ivanova, Y. Avenas, C. Schaeffer, J. B. Dezord, and J. S. Harder, "Heat pipe integrated in direct bonded copper (DBC) technology for cooling of power electronics packaging," *IEEE Trans. Power Electron.*, vol. 21, no. 6, pp. 1541–1547, Nov. 2006.

[58] S. Jahdi, O. Alatise, L. Ran, and P. Mawby, "Accurate analytical modeling for switching energy of PiN diodes reverse recovery," *IEEE Trans. Ind. Electron.*, vol. 62, no. 3, pp. 1461–1470, Oct. 2015.

[59] R. J. Wai, L. W. Liu, and R. Y. Duan, "High-efficiency voltage-clamped DC-DC converter with reduced reverse-recovery current and switch-voltage stress," *IEEE Trans. Ind. Electron.*, vol. 53, no. 1, pp. 272–280, Feb. 2006.

[60] V. P Galigekere and M K. Kazimierczuk, "Effect of SiC schottky and Si junction diode reverse recovery on boost converter," in *Proc. Electr. Insul. Conf. Electr. Manuf. Expo.*, Nashville, TN, USA, Oct. 2007, pp. 22–24.

[61] C. K. Chung, Y. J. Chen, W. M. Chen, and C. R. Kao, "Origin and evolution of voids in electroless Ni during soldering reaction," *Acta Mater.*, vol. 60, no. 11, pp. 4586–4593, Jun. 2012.

[62] J. A. Walls, "The influence of TiN ARC thickness on stress-induced void formation in tungsten-plug vias," *IEEE Trans. Power Electron.*, vol. 44, no. 12, pp. 2213–2219, Dec. 1997.

[63] Z. Chen, Y. Y. Yao, D. Boroyevich, K. D. T. Ngo, P. Mattavelli, and K. Rajashekara, "A 1200-V, 60-A SiC MOSFET multichip phase-leg module for high-temperature, high-frequency applications," *IEEE Trans. Power Electron.*, vol. 29, no. 5, pp. 2307–2320, May 2014.

[64] C. M. L. Wu, D. Q. Yu, C. M. T. Law, and L. Wang, "Properties of lead-free solder alloys with rare earth element additions," *Mater. Sci. Eng. R*, vol. 44, no. 1, pp. 1–44, Apr. 2004.

[65] K. S. Siow, "Mechanical properties of nano-silver joints as die attach materials," *J. Alloys Compounds*, vol. 514, no. 15, pp. 6–19, Feb. 2012.

[66] R. Satoh, K. Arakawa, M. Harada, and K. Matsui, "Thermal fatigue life of Pb-Sn alloy interconnections," *IEEE Trans. Compon., Hybrids, Manuf. Technol.*, vol. 4, no. 1, pp. 224–232, Oct. 2002.

[67] J. Rabkowski, G. Tolstoy, D. Peftitsis, and H. Nee, "Low-loss high-performance base-drive unit for SiC BJTs," *IEEE Trans. Power Electron.*, vol. 27, no. 5, pp. 2633–2643, May 2012.

[68] R. Vargas, U. Ammann, and J. RodrÍguez, "Predictive approach to increase efficiency and reduce switching losses on matrix converters," *IEEE Trans. Power Electron.*, vol. 24, no. 4, pp. 894–902, Feb. 2009.

[69] C. W. Lee and S. B. Park, "Design of a thyristor snubber circuit by considering the reverse recovery process," *IEEE Trans. Power Electron.*, vol. 3, no. 4, pp. 440–446, Oct. 1988.

Shancan Fu received the B.S. degree in material science and engineer from Shandong University of Science and Technology, Shandong, China, in 2009, and the M.S. degree in material science and engineer from Beihang University, Beijing, China, in 2012. He is currently working toward the Ph.D. degree at the Key Laboratory of Advanced Ceramics and Machining Technology of Ministry of Education, Tianjin University, Tianjin, China.

His current research interests include high-temperature packaging for high-power-density applications.

Yunhui Mei (M'12) received the B.S. and Ph.D. degrees in process equipment and controlling engineering from Tianjin University, Tianjin, China, in 2006 and 2010, respectively.

He studied at the Center for Power Electronics Systems, Virginia Polytechnic Institute and State University, Blacksburg, USA. He is currently an Associate Professor with the Tianjin Key Laboratory of Advanced Joining Technology and School of Material Science and Engineering, Tianjin University. He has published more than 60 papers on power electronic packaging. His current research interests include high-temperature packaging and materials for high-power-density applications.

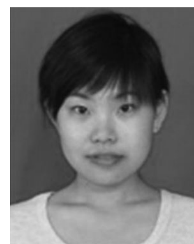

Xin Li received the B.S., M.S., and Ph.D. degrees in materials processing engineering from Tianjin University, Tianjin, China, in 2007, 2009, and 2012, respectively.

Since April 2012, she has been a Lecturer with the School of Materials Science and Engineering, Tianjin University. Her research interests include high-power electronic packaging technology and reliability.

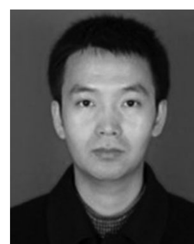

Changsheng Ma received the B.S. degree in microelectronics from Shenyang University of Technology, Shengyang, China, in 2004, respectively.

He is currently a Senior Engineer with the research and development of power electronic module, Jiangsu Macro and Micro Technology Co., Ltd, Changzhou, Jiangsu, China. He has participated several research and development in the National High Technology Research and Development Program of China. His current research interests include high-power electronics, power systems, and electric machines.

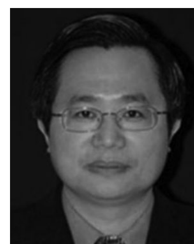

Guo-Quan Lu (M'97) received the B.S. degrees in physics and in materials science and engineering from Carnegie Mellon University, Pittsburgh, PA, USA, in 1984, and the Ph.D. degree in applied physics and materials science from Harvard University, Cambridge, MA, USA, in 1990.

He was with the Alcoa Technical Center, Alcoa Center, PA. He is currently a Professor in the Department of Materials Science and Engineering and Bradley Department of Electrical and Computer Engineering, Virginia Polytechnic Institute and State University, Blacksburg, VA, USA. He has held a Cheung Kong Guest Professorship with the Tianjin Key Laboratory of Advanced Joining Technology and the School of Material Science and Engineering, Tianjin University, Tianjin, China, since 2007. His current research interests include materials and processing development for electronic packaging of microelectronics, power electronics, and optoelectronics.

Prof. Lu received the National Science Foundation Career Award and the Research and Development 100 Award in 2007.